Journal of Hazardous Materials 321 (2017) 440–448

Contents lists available at ScienceDirect

Journal of Hazardous Materials

journal homepage: www.elsevier.com/locate/jhazmat

Inert gas influence on the laminar burning velocity of methane-air mixtures

Maria Mitu[a], Venera Giurcan[a], Domnina Razus[a,*], Dumitru Oancea[b]

[a] "Ilie Murgulescu" Institute of Physical Chemistry, 202 Spl. Independentei, Bucharest, Romania
[b] University of Bucharest, Department of Physical Chemistry, 4-12 Blvd. Elisabeta, Bucharest, Romania

HIGHLIGHTS

- Laminar burning velocities of CH_4-air-inert (He, Ar, N_2, CO_2) mixtures are reported.
- The experimental burning velocities are examined in comparison to computed ones.
- The influence of pressure and equivalence ratio on burning velocities is examined.
- The overall reaction order and overall activation energy of CH_4-O_2 reaction are reported.

ARTICLE INFO

Article history:
Received 17 June 2016
Received in revised form 25 August 2016
Accepted 14 September 2016
Available online 14 September 2016

Dedicated to the 150th anniversary of the Romanian Academy.

Keywords:
Laminar burning velocity
Methane
Inert additive
Overall activation parameters

ABSTRACT

Flame propagation was studied in methane-air-inert (He, Ar, N_2 or CO_2) mixtures with various initial pressures and compositions using pressure-time records obtained in a spherical vessel with central ignition. The laminar burning velocities of CH_4-air and CH_4-air-inert mixtures obtained from experimental $p(t)$ records of the early stage of combustion were compared with literature data and with those obtained from numerical modeling of 1D flames. The overall reaction orders of methane oxidation were determined from the baric coefficients of the laminar burning velocities determined from power-law equations. For all mixtures, the adiabatic flames temperatures were computed, assuming that the chemical equilibrium is reached in the flame front. The overall activation energy for the propagation stage of the combustion process was determined from the temperature dependence of the laminar burning velocity.

1. Introduction

The depletion of crude oil reserves and persistent requirements for cleaner combustion of fossil fuels have driven the wide use of natural gas as an alternative fuel for use in internal combustion engines (ICE) and power generation. Because the main constituent of natural gas is methane, investigation of its combustion characteristics is of great importance. Numerous studies on methane flames have focused on understanding the fundamentals of combustion in terms of ignition and extinction, propagation speed and burning velocity, dynamic behavior or instabilities, and kinetic mechanisms, among others. An important component of such studies is the determination of laminar burning velocity, which is a fundamental parameter of combustion that depends on the rate of reactions occurring in the flame and the thermo-physical properties of the flammable mixture. Numerous studies have focused on methane combustion in flames, resulting in a large body of measured and computed burning velocities at ambient initial conditions or under ICE operating conditions. Many of these data were obtained from closed vessel experiments, using synchronous records of the pressure and flame radius and applying suitable corrections for flame stretch and curvature in the early stage of combustion and for heat losses from the flame front in the late stage of combustion. A great advantage of this method is the possibility of obtaining burning velocities at pressures and temperatures different from ambient conditions. Besides this, one can evaluate the influence of pressure and temperature on the laminar burning velocity from the data of a single experiment, since the transient

* Corresponding author.
E-mail addresses: drazus@icf.ro, drazus@yahoo.com (D. Razus).

http://dx.doi.org/10.1016/j.jhazmat.2016.09.033
0304-3894/

burning velocities refer to variable temperature and pressure of the unburnt gaseous mixture [1–6]. Improved values of laminar burning velocities for CH_4-air mixtures corrected for flame stretch were reported in recent studies using outwardly propagating spherical laminar flames monitored by optical methods only a short time after ignition, when the disturbances caused by the energy input at ignition, the flame curvature, and the varying flame thicknesses are small [2,7–21]. Other models used only $p(t)$ measurements over longer periods, i.e., from ignition up to the inflection point $p(t)$ records. The laminar burning velocities of CH_4-air mixtures were determined using models for either thin flames [3,4,22,23] or thick flames [3,5,24,25]. Stationary flames anchored on burners were also used to determine the laminar burning velocity of methane with air or air + inert additives using the heat flux method [26–31]. Stagnation flames allowed determination of stretch-free laminar flame speeds of CH_4-air mixtures over extensive ranges of stoichiometry, pressure, and flame temperature [32–34]. Another recent method used data obtained in a preheated high-aspect-ratio diverging channel [35]. All recent studies delivered a reference value of $(37 \pm 1)\,cm\,s^{-1}$ for the stretch-corrected laminar burning velocity of the stoichiometric CH_4-air mixture at ambient initial conditions. For measurements at pressures and/or temperatures different from ambient conditions, a higher spread of laminar burning velocities exists despite the advanced corrections.

The wide use of natural gas as an alternative fuel has promoted numerous studies on flame propagation in methane-air mixtures diluted by inert gases because natural gas contains inert components such as N_2 or CO_2 [8,13,15,19,22–24,27,30–32,36–41]. At the same time, the use of inert gases as suppressants for methane-air explosions explains the growing number of experimental and computational studies on flame propagation and quenching. The combustion of methane in the presence of inert gases (including water (vapor)) was studied in connection to the EGR (exhaust gas recirculation) technique, which was intended to lower combustion instabilities and reduce NOx emissions and the rate of heat transfer in engines [15,39]. At the same time, the need for adequate and reliable safety recommendations have driven research on flame propagation in methane-air mixtures diluted by inert gases. Taken together, these reasons explain the growing interest in reliable values of laminar burning velocities for CH_4-air and CH_4-air-inert mixtures under various initial conditions. Recent review articles have presented the state of this problem and outlined the need to examine and improve the predictions from various chemical modeling packages by comparing the experimental and computed burning velocities [42,43].

The aim of this paper is to complete these studies with measurements of the laminar burning velocities of methane-air and methane-air diluted with He, Ar, N_2 and CO_2 determined from pressure measurements in a spherical vessel with central ignition in the early stage of flame propagation. For CH_4-air, experiments were conducted on mixtures with various initial pressures and compositions at ambient temperature. For CH_4-air-inert mixtures, experiments were performed at ambient pressure and temperature using CH_4-air with various methane-air ratios and variable inert gas contents. The laminar burning velocities obtained from experiments are compared with the burning velocities from detailed numerical modeling of 1D methane-air and methane-air-inert flames based on the GRI mechanism (version 3.0) and propagated under the same initial pressures and compositions. Using the correlations of laminar burning velocity with pressure and average flame temperature, the overall reaction orders of methane oxidation and the overall activation energy for the propagation stage of the combustion process were determined. They represent valuable input data for CFD (Computational Fluid Dynamics) modeling of flame propagation in various enclosures.

2. Experimental

Experiments were conducted in a spherical closed vessel ($V = 0.52$ L) with central ignition via inductive-capacitive sparks produced between stainless steel electrodes. A spark gap of constant width (3.5 mm) was located in the geometrical center of the spherical vessel.

The explosion was monitored using pressure measurements collected with a piezoelectric transducer Kistler 601A connected to a Charge Amplifier Kistler 5001SN coupled with an acquisition data system TestLab™ Tektronix 2505. The flame front position was determined using an ionization probe immersed at various depths in the vessel. The data acquisition was conducted at 7000 signals/s.

A vacuum and gas-feed line (which was gastight at pressures between 0.5 mbar and 5 bar) connected the explosion vessel with the gas cylinders containing fuel, air and the inert gas, the metallic cylinder for mixture storage and a vacuum pump. Before each test, the combustion vessel was evacuated to 0.5 mbar, and the explosive mixture was admitted and allowed to reach quiescence. Other details were previously reported [44–46].

CH_4-air mixtures were prepared in a 10 L storage cylinder using the partial pressure method at a total pressure of 4 bar. CH_4-air-inert mixtures were prepared directly in the combustion vessel by addition of the inert gas to any CH_4-air mixture at the appropriate partial pressures to reach the total initial pressure of 1 bar. Before ignition, the flammable mixtures were allowed to mix and become quiescent for 30 min. The average standard error observed in partial pressure measurement was 1% for CH_4 and 0.5% for inert gases.

Methane (99.99%), He (99.9999%), Ar (99.9999%), N_2 (99.99%), and CO_2 (99.99%) (SIAD Italy) were used without further purification.

Measurements using CH_4-air mixtures were collected at initial pressures between 0.5 and 2.0 bar. Measurements using CH_4-air-inert mixtures were collected at ambient initial pressure using inert concentrations within 0–40% (He, Ar, N_2) and 0–30% (CO_2) (all concentrations are given in vol/vol%).

For each experimental condition, the test was repeated 3–5 times to verify data accuracy and repeatability. The average standard error observed in explosion pressures was 2%, in the cubic law coefficients was 2.5% and was less than 3.5% in the corresponding burning velocities.

3. Computing program

The adiabatic flame temperatures and adiabatic explosion pressure of flammable mixtures were calculated using the COSILAB 0-D program [47] with the assumption that the thermodynamic equilibrium is reached within the flame. This program is based on a general algorithm for computing the equilibrium composition of products for fuel-oxidizer gaseous mixtures by determining the minimum of the free enthalpy (isobaric combustion) or free energy (isochoric combustion).

Kinetic modeling of one-dimensional, premixed laminar free flames was performed with the COSILAB 1-D package (version 3.0.3) which uses preprocessors that accept molecular and thermodynamic data and reaction mechanisms compatible to the international standard format put forward by Sandia National laboratories. As solvers, the package uses a steady Newton solver (usually 25 iterations, relative tolerance 10^{-5}; absolute tolerance 10^{-8}), an unsteady Newton solver (usually 15 iterations, relative tolerance 10^{-4}; absolute tolerance 10^{-6}) and an unsteady Euler solver. For the adaptive grid parameters, we used GRAD = 0.1, CURV = 0.2 and maximum ratio of adjacent cell size between 1.3 and 1.1. The modeling used GRI (Gas Research Institute) mechanism version 3.0 [47]. This mechanism, in which 53 chemical species and

325 elementary reactions are considered, was optimized for combustion of natural gas in air. The computations were performed for premixed 1D adiabatic laminar free flames of methane-air at various initial compositions ([CH_4] = 6.0–12.0%) and pressures (0.5–2 bar) and for methane-air-inert mixtures at various initial compositions ([CH_4] = 6.0–12.0%; [inert] = 5–30%) and ambient initial pressure.

4. Data evaluation

The laminar burning velocity was calculated from the cubic law coefficient of pressure rise in the early stage of flame propagation in a closed vessel k by assuming isothermal compression of unburned gas ahead the flame front [44]:

$$S_u = R \cdot \left(\frac{k}{\Delta p_{max}}\right)^{1/3} \left(\frac{p_0}{p_{max}}\right)^{2/3} \quad (1)$$

where R is the radius of the explosion vessel, Δp_{max} is the peak pressure rise of the explosion at the initial pressure p_0, and $p_{max} = \Delta p_{max} + p_0$. The measured values of p_{max} and Δp_{max} were used as input values for S_u calculation.

The cubic law coefficient, given by equation:

$$\Delta p = kt^3 \quad (2)$$

was determined for each experiment using a nonlinear regression method with a relationship of the form:

$$\Delta p = a + k \cdot (t - c)^3 \quad (3)$$

where a and c are corrections for pressure and time, respectively, necessary for eliminating the signal shift of the pressure transducer and the possible delay in signal triggering [44]. The cubic law coefficient was obtained for each experiment over a restricted pressure range of

$$p_0 \le p \le 2\,p_0.$$

From Eqs. (1)–(3), it can be observed that the method requires only measurable properties and can be applied to mixtures of unknown nature and composition.

5. Results and discussion

5.1. Methane-air

The laminar burning velocities of methane-air at various initial pressures and ambient initial temperature are plotted against methane concentration in Fig. 1 along with the best-fit correlations of data as 2nd order polynomials. The plot displays a broad peak near the stoichiometric concentration ([CH_4] = 9.5%) for all examined pressures. The smoothed peak burning velocity at 1 bar is $S_u = 39\,cm\,s^{-1}$, which is well within the range of values reported from the literature. The initial pressure increase results in the decrease of laminar burning velocities for all examined mixtures. Several data sets referring to lean and stoichiometric CH_4-air mixtures are shown in Fig. 2.

A comparison between the laminar burning velocities of methane-air at ambient initial conditions from the current measurements and from the literature based on various experimental techniquesis shown in Fig. 3. The data were fitted by 2nd order polynomials, also plotted in Fig. 3. The current results are close to the stretch-corrected burning velocities reported by Liao from measurements on outwardly propagating flames [9] but are higher compared with data reported by other authors using stationary flames and heat flux measurements [28] or counterflow flames [33]. The burning velocities of methane-air at ambient initial conditions obtained from 2nd order polynomial fit of data from various authors, together with other measured burning velocities reported in literature are listed in Table 1. Even when the measured data were corrected for stretch in the incipient stage of the propagation and for other disturbing effects, the laminar burning velocities at ambient initial conditions are scattered within 34.0 and

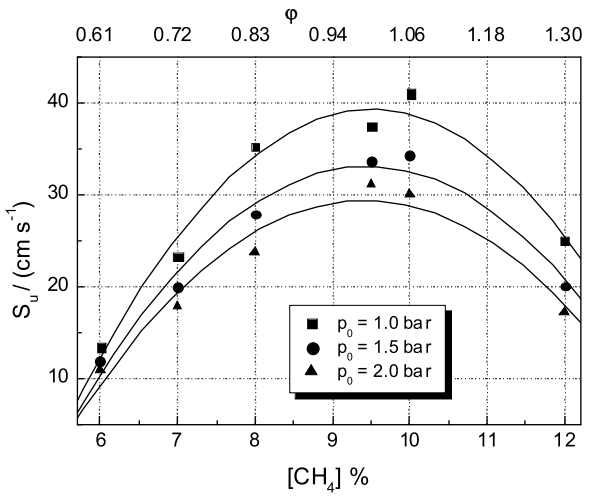

Fig. 1. Laminar burning velocities of CH_4–air at various initial pressures; experimental data.

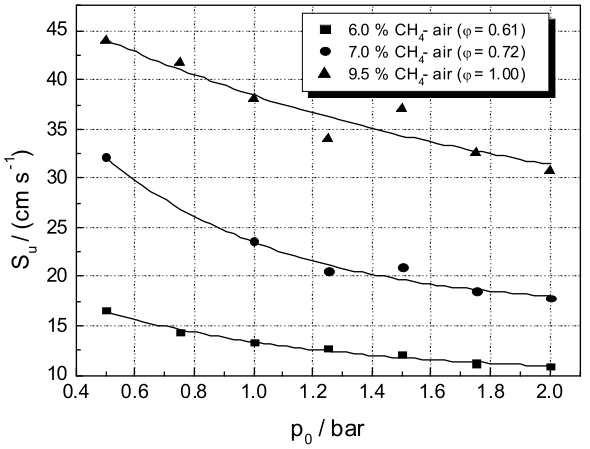

Fig. 2. Pressure influence on laminar burning velocities of CH_4–air; experimental data.

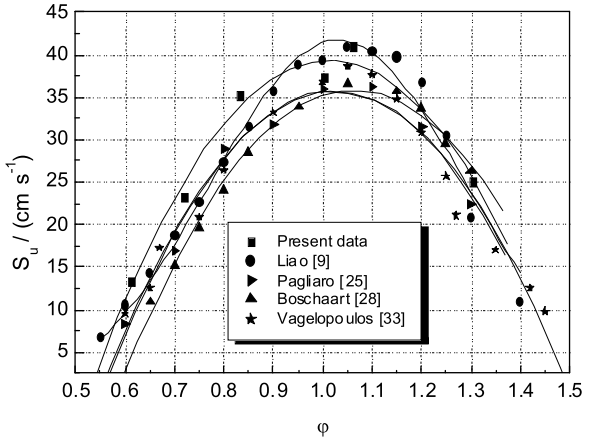

Fig. 3. Laminar burning velocities of CH_4–air at ambient initial conditions; present experimental data and reference values from literature: outwardly propagating flames [9,25]; flat flames, heat flux technique [28]; counterflow flames [33].

Table 1
Reference values of laminar burning velocities for stoichiometric CH_4-air mixtures at T_0 = 298 K and p_0 = 1 bar.

Measuring conditions	S_u/(cm s^{-1})	Refs.
OPF (outwardly propagating spherical flames);	33.9	Hassan et al. [2]
synchronous measurements of p(t) and r_{fl}(t)	39.4	Liao et al. [9]
	35.0	Rozenchan et al. [8]
	34.6	Halter et al. [11,13,14], Galmiche et al. [15]
	34.5	Liang et al. [19]
Spherical vessel, p(t) records; thin-flame model	41.0	Zhang et al. [23]
Spherical vessel, p(t) records; multi-zone flame model	35.0	Han et al. [39]
Heat flux measurement, stretch-corrected	37.0	van Maaren et al. [26]
burning velocities	36.6	Boschaart and de Goey [28]
	35.9	Goswami et al. [29]
Counter-flow opposed twin-jet flames	35.0	Zhu et al. [32]
	36.8	Vagelopoulos and Egolfopoulos [33]
Single jet flame (single jet-plate configuration)	35.7	Park et al. [34]

Table 2
Baric coefficients ν of laminar burning velocities for CH_4-air mixtures at 298 K.

[CH_4] %	6.0	7.0	8.0	9.5	10.0	12.0
φ[a]	0.61	0.72	0.83	1.00	1.06	1.30
$-\nu$	0.296	0.393	0.578	0.264	0.448	0.550

[a] φ is the equivalence ratio defined as $\varphi = ([CH_4]/[O_2])/([CH_4]/[O_2])_{stoich}$.

Table 3
Reference values of baric coefficient ν for stoichiometric CH_4-air mixtures at 298 K.

Pressure range (bar)	$-\nu$	Reference
1–8	0.30	Hill and Hung [48]
1–10	0.37	Gu et al. [7]
0.75–70	0.44	Elia et al. [37]
1–10	0.28	Dahoe and de Goey [3]
0.5–1.5	0.40	Liao et al. [9]
1–5	0.37	Han et al. [39]
1–5	0.38	Goswami et al. [29]
1–60	0.32[a]	Hu et al. [21]

[a] The authors report a decrease of the baric coefficient with pressure increase within 1–60 bar.

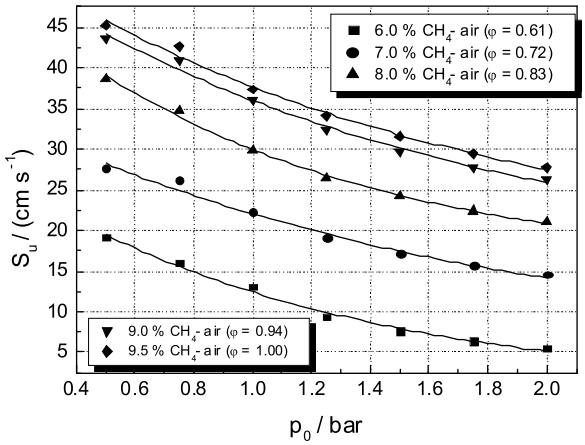

Fig. 4. Pressure influence on laminar burning velocities of CH_4–air; computed data.

41.0 cm s^{-1}. In recent discussions of discrepancies between these values and the main error sources, Chen [20] and Egolfopoulos [43] acknowledged that the uncertainty in laminar burning velocities for methane-air measurements using spherical flames is approximately 5% for systems at ambient initial pressure and temperature but might increase to 8–10% for mixtures at different initial conditions. Based on this observation, the current measurements can be used in further examination of the inert gas influence on the laminar burning velocities of methane-air.

The pressure dependence of the laminar burning velocities for methane-air was examined using a power law:

$$S_u = S_{u,ref}\left(\frac{p}{p_0}\right)^{\nu} \quad (4)$$

where $S_{u,ref}$ is the laminar burning velocity at reference pressure p_{ref}, and ν is the baric coefficient. In the current case, p_{ref} was 1 bar. The baric coefficients of the laminar burning velocities determined by a non-linear regression analysis of $S_{u,ref}$ versus p data are given in Table 2. The negative values indicate a decrease of S_u when p increases. For the stoichiometric CH_4-air mixture, we found $\nu = -0.264$, which is close to the values reported by Dahoe at al. [3] and Hill [48] from measurements performed using the spherical vessel technique over an extended pressure range, as given in Table 3. The baric coefficients for lean and rich CH_4-air mixtures are lower compared with the stoichiometric mixture. No definite trend is noted between the baric coefficient and the equivalence ratio.

A comparison of the measured and predicted laminar burning velocities can be useful in revealing the issues associated with these results. The pressure influence on the laminar burning velocity predicted by modeling is shown in Table 4 and Fig. 4. A comparison of the laminar burning velocities measured and predicted by the GRI 3.0 mechanism is also given in Table 4. The computed burning velocities are systematically lower than the measured values, but the variation trend is the same for both data sets, i.e., the peak burning velocity appears at 10% (rich CH_4-air mixture) at ambient initial pressure and at 9.5% (stoichiometric CH_4-air composition) at p_0 = 2.0 bar.

The influence of pressure on the laminar burning velocity can be understood by examining the relationship derived in the thermal theory of flame propagation [49]:

$$S_u \sim \left(\frac{\lambda}{\rho C_p}\cdot C_0^{1-n}\cdot \exp(-E_a/RT_f)\right)^{1/2} \quad (5)$$

where λ is the thermal conductivity, ρ – density and C_p – specific heat of unburned gas; C_0 is the initial fuel concentration, T_f is the end temperature of the flame front, and n and E_a are the overall activation parameters (reaction order and activation energy, respectively) of the oxidation reaction.

At constant fuel concentration, the pressure increase should result in an increase in the density and a decrease in the laminar burning velocity. The other properties, such as the thermal conductivity and specific heat, appear to be less influenced by pressure [50]. The overall pressure effect on the laminar burning velocity expressed by the baric coefficient ν can be further used to determine the overall reaction order n. This analysis is presented in Section 5.3.

Table 4
Experimental and computed burning velocities of CH_4-air at two pressures.

$[CH_4]$ %	φ	p_0 = 1.0 bar		p_0 = 2.0 bar	
		$S_{u,exp}$/(cm s^{-1})	$S_{u,calc}$/(cm s^{-1})	$S_{u,exp}$/(cm s^{-1})	$S_{u,calc}$/(cm s^{-1})
6.0	0.609	13.4	13.0	10.9	5.5
7.0	0.719	23.3	22.1	17.7	14.5
8.0	0.830	35.2	29.8	23.6	21.0
9.0	0.944	–	35.9	–	26.2
9.5	1.002	37.4	37.4	31.2	27.8
10.0	1.061	41.0	38.4	30.1	30.6
11.0	1.180	–	35.2	–	25.0
12.0	1.302	25.0	24.6	17.1	15.4

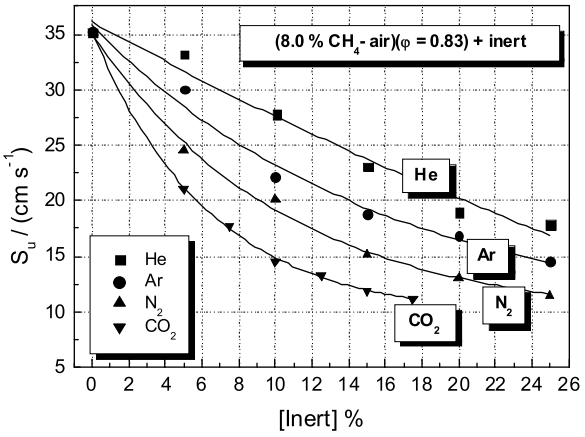

Fig. 5. Influence of inert gas addition on the laminar burning velocities of a lean CH_4–air mixture; experimental data.

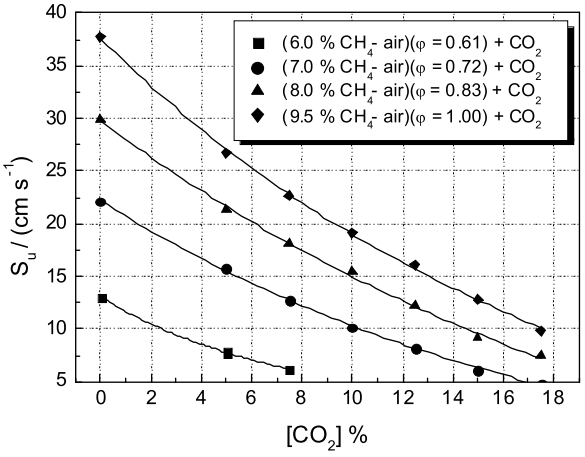

Fig. 6. CO_2 influence on computed burning velocities of lean- and stoichiometric CH_4–air mixtures.

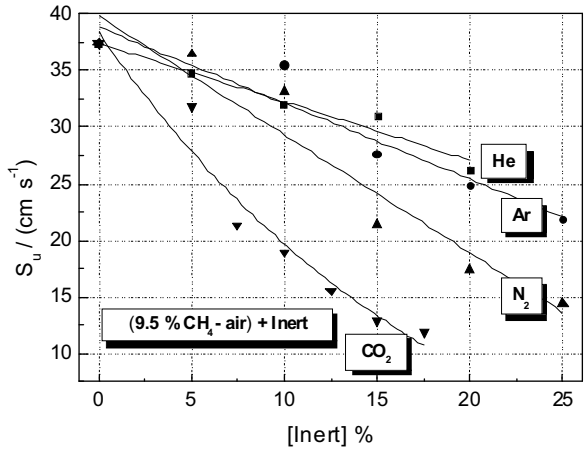

Fig. 7. Comparison between experimental and computed burning velocities of stoichiometric CH_4–air–inert mixtures.

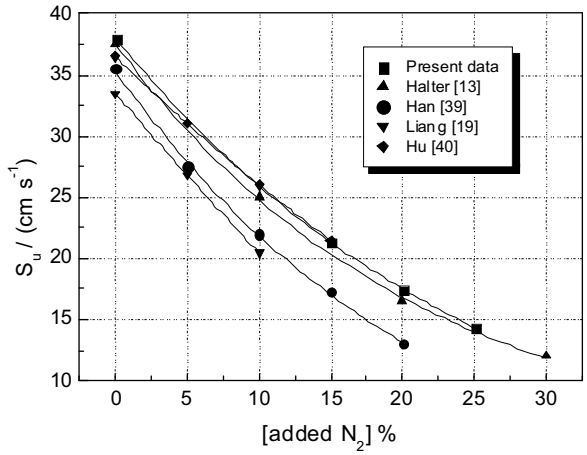

Fig. 8. Nitrogen influence on burning velocities for the stoichiometric CH_4–air mixture at ambient initial pressure and temperature.

5.2. Methane-air-inert mixtures

The laminar burning velocities of methane-air-inert mixtures at 300 K obtained from the experiments are plotted in Fig. 5, where a comparison of the inert additive influence is shown. For all methane-air mixtures, CO_2 has the greatest influence on burning velocity, followed by N_2, Ar and He. A similar variation is observed for the computed laminar burning velocities. Typical plots are shown in Fig. 6 for CH_4-air-CO_2 mixtures.

A comparison of experimental and computed data is shown in Fig. 7, where the lines represent the computed burning velocities. The experimental burning velocities are scattered around the computed burning velocities, but their variation with the inert gas concentration is consistent with the expected trend: inert gas addition determines the burning velocity decrease.

The influence of inert gas addition on the laminar burning velocity of methane-air mixtures was examined by many authors using both experimental and computational methods [13,15,19,22–24,27,30–32,36–41,51,52]. Plots of the current experimental data compared with the reference burning velocities from literature are shown in Figs. 8 and 9. Our data on N_2- and CO_2-diluted stoichiometric CH_4-air mixtures are similar to those reported by Halter et al. [13] and Hu [40] as stretch-corrected data for outwardly propagating spherical flames. No direct comparison could be made with the burning velocities of Ar-diluted CH_4-air mixtures reported by Zhang et al. [23] and with the burning veloc-

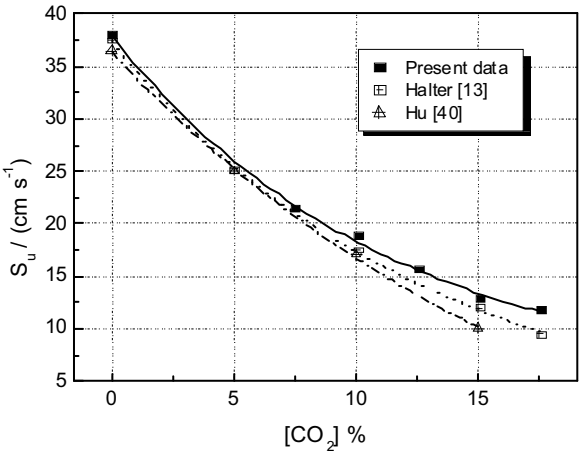

Fig. 9. CO_2 influence on burning velocities for the stoichiometric CH_4–air mixture at ambient initial pressure and temperature.

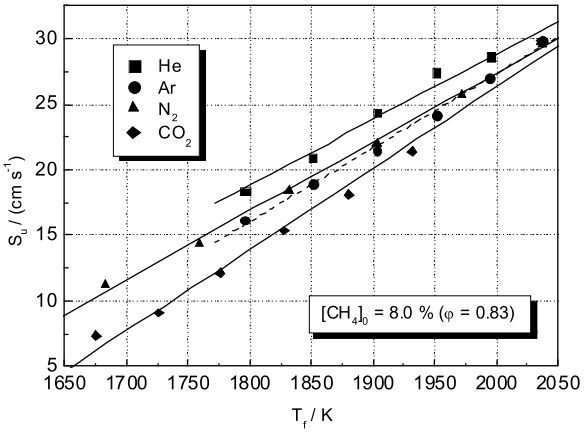

Fig. 10. Correlation between the laminar burning velocities and the adiabatic flame temperatures for lean methane–air–inert mixtures.

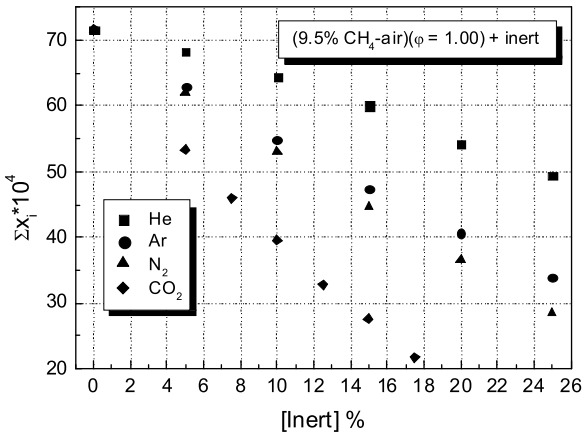

Fig. 11. Variation of total peak mass fraction for radical species against inert gas concentration; stoichiometric methane–air–inert mixtures.

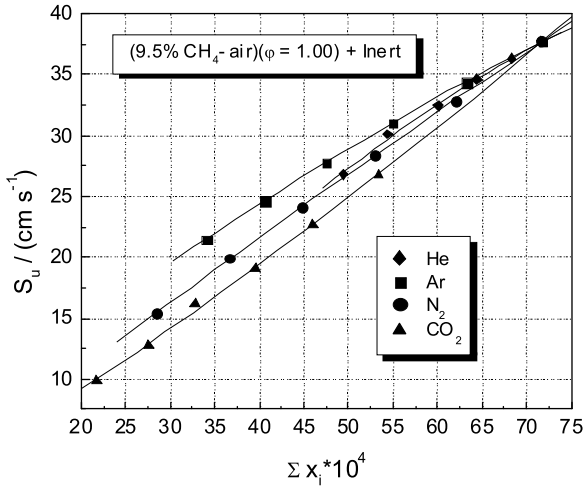

Fig. 12. Variation of laminar burning velocities versus the total peak mass fraction for radical species; stoichiometric methane–air–inert mixtures.

ities of CO_2-diluted CH_4-air mixtures, reported by Qin et al. [52]. These datasets couldn't be compared directly because the algorithm for computing their composition was different. In the cited papers [23,52] the inert concentration was expressed as% from the initial amount of (CH_4 + inert) whereas in our measurements the inert concentration was expressed as% from the total gas amount (CH_4 + inert +air).

The influence of inert additives on laminar burning velocity was assigned mostly to their ability to change the thermal properties of flammable mixtures by changing the heat capacity and consequently the flame temperature. Indeed, the laminar burning velocities correlate well with the adiabatic flame temperatures, as shown in Fig. 10 for certain representative mixtures. The effect of dilution by inert gases on maximum flame temperature varies in the order of $CO_2 > N_2 \cong Ar > He$. Additionally, inert addition determines the decrease in fuel content (resulting in the decrease of the available amount of released heat and the reaction rate) and influences both the thermal diffusivity of the reacting mixture and the oxidation reaction kinetics [49,50]. The differences in thermal diffusivities are observed by examining CH_4-air flames diluted by He and Ar gases with the same heat capacity. Overall, Ar, with a higher molecular weight than He, has a lower thermal diffusivity, resulting in lower burning velocities for Ar-diluted mixtures compared with He-diluted mixtures. In the case of CO_2 dilution, a specific influence exists based on its ability to dissociate and to dissipate heat by radiation.

A quantitative evaluation of the physical and chemical effects of each additive has been recently reported [13,15,38,40] by considering the flame propagation of "real" and "false" additive molecules (FHe, FAr, FN_2, and FCO_2) in modeling, i.e., molecules that have the same thermal and transport characteristics as their corresponding "real" molecules but do not participate in any reaction. For any additive, e.g., CO_2, the chemical effect of its addition is shown by the difference between the results of CO_2 and FCO_2. Halter [13] showed that the burning velocities of CH_4-air-FCO_2 are located between those corresponding to dilution with N_2 and CO_2, but the effect of carbon dioxide dissociation is less important when the additive amount is increased because the flame temperature is lower and does not afford extensive dissociation.

The variation of laminar burning velocities determined by addition of inert gases to methane-air changes in parallel with the decrease of the peak mass fraction of reactive radical species in the front of these flames. Taking H, OH, O and HO_2 as representative species, the plots of Σx_i (the sum of their peak mass fractions) versus inert concentration given in Fig. 11 are similar to those in Fig. 7, where the burning velocities were plotted against inert concentration. In Fig. 12, the burning velocities are shown as functions of Σx_i for stoichiometric CH_4-air-inert mixtures. Among the examined cases, CH_4-air-He mixtures have the highest concentration of reactive radical species and CH_4-air-CO_2 mixtures have the lowest, in accordance with their flame temperatures.

Table 5
Sum of peak mass fractions for the most important radical species and volumetric rates of heat release at T = ct = 1700 K; stoichiometric CH_4-air diluted with 10% inert gas.

Inert	$\Sigma x_i * 10^4$	$-R_{max}$ (Maximum volumetric rate of heat release)·10^{-8}/(J s^{-1} m^{-3})	S_u/(cm s^{-1})
He	24.01	30.7	34.59
Ar	19.72	28.9	31.08
N_2	22.01	23.6	28.35
CO_2	27.43	6.46	19.14

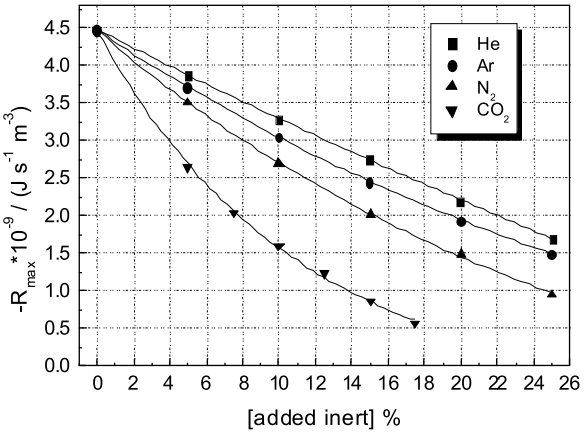

Fig. 13. Influence of inert gas concentration on the maximum rate of heat release; stoichiometric methane–air–inert mixtures.

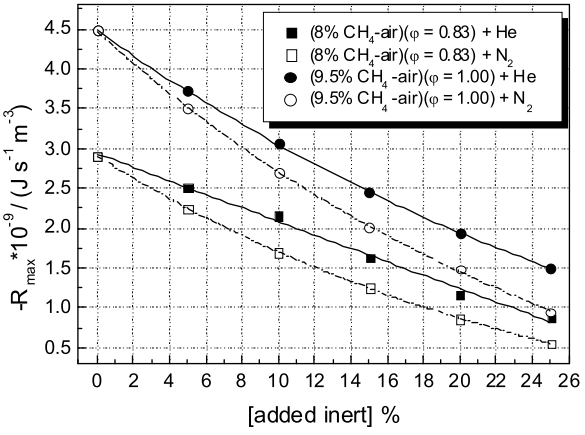

Fig. 14. Inert gas influence on the maximum rate of heat release; lean– and stoichiometric methane–air–inert mixtures.

Examining several methane-air-inert systems with constant CH_4 and inert concentrations and choosing the same flame temperature across the reaction zone, the mixtures containing CO_2 show the lowest rate of heat release and the lowest laminar burning velocity but the highest mass fraction of radicals. A set of representative data given in Table 5 confirms the combined influence of carbon dioxide on flame propagation via a lower heat release rate and extended dissociation in the flame front, resulting in lower laminar burning velocities. Comparison of data referring to other inert additives confirms the variation of laminar burning velocities given in Fig. 12.

The influence of additive concentration on the maximum volumetric rates of heat release is shown in Fig. 13 for stoichiometric CH_4-air diluted by various amounts of inert gases. Similar data referring to lean CH_4-air-inert mixtures compared with the stoichiometric CH_4-air-inert mixtures are plotted in Fig. 14. The plots are quite similar to those from Fig. 5 and 6 in which the dependence of laminar burning velocities on inert concentration is shown.

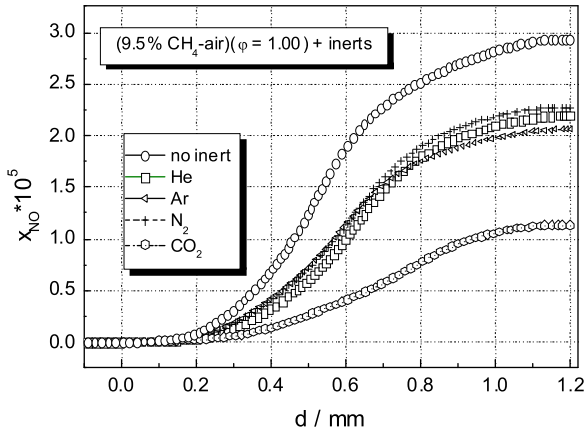

Fig. 15. NO mass fraction in the flame front of stoichiometric methane–air mixtures diluted by 10% inert gas.

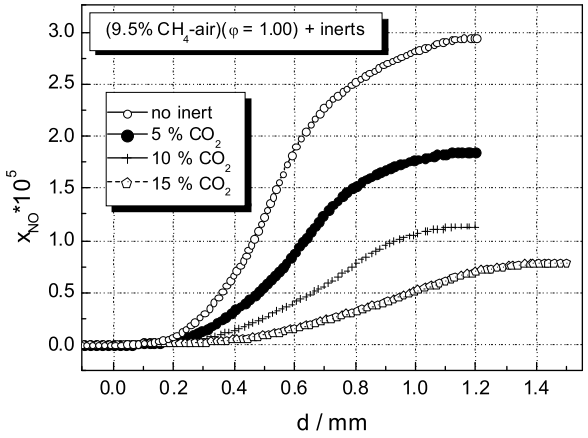

Fig. 16. NO mass fraction in the flame front of stoichiometric methane–air mixtures diluted by various CO_2 amounts.

The modeling of flame propagation also yields valuable information on pollutant formation and concentration variation depending on the operational variables. Inert gas addition results in the decrease of NO concentration, as shown in Figs. 15 and 16 by the concentration profiles of NO across flames of the stoichiometric CH_4-air-inert mixtures compared with those of the non-diluted CH_4-air mixture.

Among the studied additives, CO_2 determines the larger variation of [NO], as observed from Fig. 15. The increase of [CO_2] in mixtures with the same initial methane concentration results in the decrease of [NO], as shown in Fig. 16. The decrease of [NO] in the burned gas as a result of CO_2 addition to CH_4-air mixtures has been assigned primarily to temperature decrease determined by dilution, and this effect explains the beneficial influence of exhaust gas recirculation on NOx decrease in emissions of automotive engines.

Table 6
Overall reaction orders n of methane oxidation in CH_4-air flames.

$[CH_4]$ %	6.0	7.0	8.0	9.5	10.0	12.0
φ	0.61	0.72	0.83	1.00	1.06	1.30
n	1.41	1.21	0.84	1.47	1.10	0.90

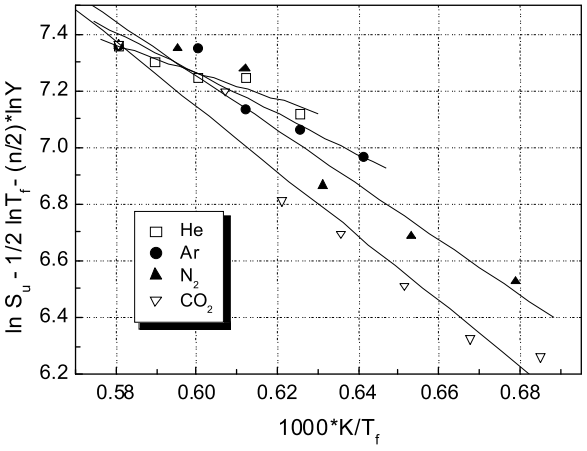

Fig. 17. Variation of experimental burning velocities against average flame temperatures for stoichiometric CH_4–air–inert mixtures.

5.3. Overall kinetic parameters of methane-oxygen reaction in laminar flames

From the baric coefficients ν of the methane-air burning velocities, the overall reaction orders n can be obtained using the relationship [49,53]:

$$n = 2(\nu + 1) \quad (6)$$

Representative values of the overall reaction orders are given in Table 6 and range among values reported for methane-air mixtures at ambient initial temperature, between 0.84 and 1.5 [8,21,32]. It must be noted that our data, which were obtained from laminar burning velocities determined over a restricted pressure range within 0.5 and 2.0 bar, produced constant baric coefficients and overall reaction orders for the mentioned pressure range. In contrast, other authors (Egolfopoulos [32]; Rozenchan [8]; Goswami [29]) found that overall reaction orders depended on the pressure range in which the data were obtained.

According to Eq. (6), the laminar burning velocity is directly influenced by the overall reaction rate in the flame front, and therefore, the good correlation of laminar burning velocities with flame temperatures illustrated by the data in Fig. 10 can be used to evaluate the overall activation energy of the combustion process. The overall activation energy of methane-oxygen reaction in the flame front of methane-air-inert mixtures was calculated using a modified Arrhenius type equation [54] after assuming that the flame can be modeled using a single-step process:

$$\ln S_u - \frac{1}{2}\ln \overline{T_f} - \frac{n}{2}\ln Y = Const. - \frac{E_a}{2R\overline{T_f}} \quad (7)$$

where Y is the mole fraction of reactive components (fuel + oxidant) in the mixture, n is the overall reaction order and $\overline{T_f}$ is the average temperature within the flame front defined as [54]:

$$\overline{T_f} = T_0 + 0.74 \cdot (T_f - T_0) \quad (8)$$

Fig. 17 displays plots of the left member of Eq. (7) versus the reciprocal average flame temperature for the stoichiometric methane-air mixture diluted with He, Ar, N_2 and CO_2. The activation energies obtained from the slopes of linear correlations (7) using the overall reaction orders n from Table 6 are given in Table 7 for mixtures with variable methane concentration.

Table 7
Overall activation energies E_a of methane oxidation in inert-diluted CH_4-air flames.

$[CH_4]_0$%	φ	E_a/(kJ/mol)			
		He	Ar	N_2	CO_2
7.0	0.72	49 ± 9	79 ± 17	64 ± 16	54 ± 22
8.0	0.83	99 ± 20	128 ± 8	123 ± 11	121 ± 14
9.5	1.00	79 ± 15	120 ± 22	160 ± 20	190 ± 17
10.0	1.06	146 ± 62	160 ± 24	161 ± 16	174 ± 189

The overall activation energies of the methane-oxygen reaction in the presence of inert components range within the typical values characteristic for fuel-oxidant-inert mixtures: E_a = 134 kJ/mol for stoichiometric ethylene-air-Ar mixtures, 159 kJ/mol for ethylene-air-CO_2 and 97 kJ/mol for ethylene-air-N_2 [55]. For stoichiometric propene-air-inert mixtures, we found that E_a = 146 kJ/mol (dilution by Ar) and E_a = 207 kJ/mol (dilution by CO_2) [56]. Among the examined additives for the stoichiometric methane-, ethylene- and propene-air mixtures, the highest activation energies were calculated for CO_2-diluted fuel-air mixtures.

6. Conclusions

Flame propagation during deflagration of stoichiometric methane-air mixtures diluted with various inerts (He, Ar, N_2, CO_2) in a spherical vessel with central ignition was monitored using pressure measurements. The laminar burning velocities were calculated from pressure-time records in the early stage of spherical propagation.

The experimental laminar burning velocities are examined compared with the computed burning velocities that were obtained from a numerical modeling of 1D laminar flames using the GRI version 3.0 mechanism. For all data, the diluent influence on burning velocities is discussed. The burning velocities obtained from detailed modeling of combustion using the program COSILAB display underestimated values compared with both the current measured velocities and other literature data. The fair agreement between the experimental burning velocities and reference values from the literature confirms the possibility of using the actual simple method for extracting the laminar burning velocities from experimental measurements of transient pressure in the early stage of explosion propagation.

A strong influence of the inert additives on the laminar burning velocity, maximum flame temperature, and concentration of active radical species in the flame front was observed. Dilution with increasing amounts of additives determines the decrease of laminar burning velocity and maximum flame temperature for all investigated compositions of the methane-air mixtures. Among the studied additives, CO_2 is the most efficient, followed by N_2, Ar and He. The results are attributed to the higher heat capacity and heat dissipation rate of carbon dioxide compared with nitrogen, argon and helium. The dilution effect is also observed in the overall activation energy of the stoichiometric CH_4-air mixture, i.e., 190 kJ/mol (CH_4-air-CO_2), 160 kJ/mol (CH_4-air-N_2), 120 kJ/mol (CH_4-air-Ar) and 79 kJ/mol (CH_4-air-He), relevant values of the inert effect of carbon dioxide on flame propagation in methane-air mixtures.

References

[1] G. Andrews, D. Bradley, The burning velocity of methane-air mixtures, Combust. Flame 19 (1972) 275–288.

[2] M.I. Hassan, K.T. Aung, G.M. Faeth, Measured and predicted properties of laminar premixed methane/air flames at various pressures, Combust. Flame 115 (1998) 539–550.
[3] A.E. Dahoe, L.P.H. de Goey, On the determination of the laminar burning velocity from closed vessel gas explosions, J. Loss Prev. Process Ind. 16 (2003) 457–478.
[4] F. Cammarota, A. Di Benedetto, V. Di Sarli, E. Salzano, G. Russo, Combined effects of initial pressure and turbulence on explosions of hydrogen-enriched methane/air, mixtures, J. Loss Prev. Process Ind. 22 (2009) 607–613.
[5] S.P. Marshall, R. Stone, C. Hegheş, T.J. Davies, R.F. Cracknell, High pressure laminar burning velocity measurements and modelling of methane and n-butane, Comb. Theory Model. 14 (2010) 519–540.
[6] A.M. Garforth, C.J. Rallis, Laminar burning velocity of stoichiometric methane-air: pressure and temperature dependence, Combust. Flame 31 (1978) 53–68.
[7] X.J. Gu, M.Z. Haq, M. Lawes, R. Woolley, Laminar burning velocity and Markstein lengths of methane–air mixtures, Combust. Flame 121 (2000) 41–58.
[8] G. Rozenchan, D.L. Zhu, C.K. Law, S.D. Tse, Outward propagation burning velocities, and chemical effects of methane flames up to 60 atm, Proc. Combust. Inst. 29 (2002) 1461–1469.
[9] S.Y. Liao, D.M. Jiang, Q. Cheng, Determination of laminar burning velocities for natural gas, Fuel 83 (2004) 1247–1250.
[10] C.K. Law, O.C. Kwon, Effects of hydrocarbon substitution on atmospheric hydrogen–air flame propagation, Int. J. Hydrogen Energy 29 (2004) 867–879.
[11] F. Halter, C. Chauveau, N. Djebaili-Chaumeix, I. Gökalp, Characterization of the effects of pressure and hydrogen concentration on laminar burning velocities of methane–hydrogen–air mixtures, Proc. Combust. Inst. 30 (2005) 201–208.
[12] Z. Huang, Y. Zhang, K. Zeng, B. Liu, Q. Wang, D. Jiang, Measurements of laminar burning velocities for natural gas–hydrogen–air mixtures, Combust. Flame 146 (2006) 302–311.
[13] F. Halter, F. Foucher, L. Landry, C. Mounaïm-Rousselle, Effect of dilution by nitrogen and/or carbon dioxide on methane and iso-octane air flames, Combust. Sci. Technol. 181 (2009) 813–827.
[14] F. Halter, T. Tahtouh, C.M. Rousselle, Nonlinear effects of stretch on the flame front propagation, Combust. Flame 157 (2010) 1825–1832.
[15] B. Galmiche, F. Halter, F. Foucher, P. Dagaut, Effects of dilution on laminar burning velocity of premixed methane/air flames, Energy Fuels 25 (2011) 948–954.
[16] Z. Chen, On the extraction of laminar flame speed and Markstein length from outwardly propagating spherical flames, Combust. Flame 158 (2011) 291–300.
[17] E. Varea, V. Modica, A. Vandel, B. Renou, Measurement of laminar burning velocity and Markstein length relative to fresh gases using a new postprocessing procedure: application to laminar spherical flames for methane, ethanol and isooctane/air mixtures, Combust. Flame 159 (2012) 577–590.
[18] C.H. Osorio, A.J. Vissotski, E.L. Petersen, M.S. Mannan, Effect of CF_3Br on C1–C3 ignition and laminar flame speed: numerical and experimental evaluation, Combust. Flame 160 (2013) 1044–1059.
[19] Y.T. Liang, W. Zeng, E.J. Hu, Experimental study of the effect of nitrogen addition on gas explosion, J. Loss Prev. Process Ind. 26 (2013) 1–9.
[20] Z. Chen, On the accuracy of laminar flame speeds measured from outwardly propagating spherical flames: methane/air at normal temperature and pressure, Combust. Flame 162 (2015) 2442–2453.
[21] E. Hu, X. Li, X. Meng, Y. Chen, Y. Cheng, Y. Xie, Z. Huang, Laminar flame speeds and ignition delay times of methane–air mixtures at elevated temperatures and pressures, Fuel 158 (2015) 1–10.
[22] A. Di Benedetto, V. Di Sarli, E. Salzano, F. Cammarota, G. Russo, Explosion behavior of CH4/O2/N2/CO2 and H2/O2/N2/CO2 mixtures, Int. J. Hydrogen Energy 34 (2009) 6970–6978.
[23] B. Zhang, G. Xiu, C. Bai, Explosion characteristics of argon/nitrogen diluted natural gas–air mixtures, Fuel 124 (2014) 125–132.
[24] N. Hinton, R. Stone, Laminar burning velocity measurements of methane and carbon dioxide mixtures (biogas) over wide ranging temperatures and pressures, Fuel 116 (2014) 743–750.
[25] J.L. Pagliaro, G.T. Linteris, P.B. Sunderland, P.T. Baker, Combustion inhibition and enhancement of premixed methane–air flames by halon replacements, Combust. Flame 162 (2015) 41–49.
[26] A. van Maaren, D.S. Thung, L.R.H. De Goey, Measurement of flame temperature and adiabatic burning velocity of methane/air mixtures, Combust. Sci. Technol. 96 (1994) 327–344.
[27] I.V. Dyakov, A.A. Konnov, J.D. Ruyck, K.J. Bosschaart, E.C.M. Brock, L.P.H. De Goey, Measurement of adiabatic burning velocity in methane-oxygen-nitrogen mixtures, Combust. Sci. Technol. 172 (2011) 81–96.
[28] K.J. Bosschaart, L.P.H. de Goey, The laminar burning velocity of mixtures of hydrocarbon and air as measured with the heat-flux method, Combust. Flame 136 (2004) 261–269.
[29] M. Goswami, S.C.R. Derks, K. Coumans, W.J. Slikker, M.H. de Andrade Oliveira, R.J.M. Bastiaans, C.M. Luijten, L.P.H. de Goey, A.A. Konnov, The effect of elevated pressures on the laminar burning velocity of methane + air mixtures, Combust. Flame 160 (2013) 1627–1635.
[30] P. Zahedi, K. Yousefi, Effects of pressure and carbon dioxide, hydrogen and nitrogen concentration on laminar burning velocities and NO formation of methane-air mixtures, J. Mech. Sci. Technol. 28 (2014) 377–386.
[31] Y.L. Chan, M.M. Zhu, Z.Z. Zhang, P.F. Liu, D.K. Zhang, The Effect of CO2 dilution on the laminar burning velocity of premixed methane/air flames, Energy Procedia 75 (2015) 3048–3053.
[32] D. Zhu, F. Egolfopoulos, C.K. Law, Experimental and numerical determination of laminar flame speeds of methane (Ar, N_2 CO_2)-air mixtures as function of stoichiometry, pressure and flame temperature, 22nd Symposium (International) on Combustion (1989) 1537–1545.
[33] C.M. Vagelopoulos, F.N. Egolfopoulos, Direct experimental determination of laminar flame speeds, Proc. Combust. Inst. 27 (1998) 513–519.
[34] O. Park, P.S. Veloo, N. Liu, F.N. Egolfopoulos, Combustion characteristics of alternative gaseous fuels, Proc. Combust. Inst. 33 (1) (2011) 887–894.
[35] M. Akram, P. Saxena, S. Kumar, Laminar burning velocity of methane–air mixtures at elevated temperatures, Energy Fuels 27 (2013) 3460–3466.
[36] R. Stone, A. Clarke, P. Beckwith, Correlations for the laminar-burning velocity of methane/diluent/air mixtures obtained in free-fall experiments, Combust. Flame 114 (1998) 546–555.
[37] M. Elia, M. Ulinski, M. Metghalchi, Laminar burning velocity of methane–air–diluent mixtures, J. Eng. Gas Turbines Power 123 (1) (2000) 190–196.
[38] F. Liu, H. Guo, G.J. Smallwood, The chemical effect of CO2 replacement of N2 in air on the burning velocity of CH_4 and H_2 premixed flames, Combust. Flame 133 (2003) 495–497.
[39] P. Han, M.D. Checkel, B.A. Fleck, N.L. Nowicki, Burning velocity of methane/diluent mixture with reformer gas addition, Fuel 86 (2007) 585–596.
[40] E. Hu, X. Jiang, Z. Huang, N. Iida, Numerical study on the effects of diluents on the laminar burning velocity of methane-air mixtures, Energy Fuels 26 (2012) 4242–4252.
[41] J. Sidey, E. Mastorakos, R.L. Gordon, Simulations of autoignition and laminar premixed flames in methane/air mixtures diluted with hot products, Combust. Sci. Technol. 186 (2014) 453–468.
[42] E. Ranzi, A. Frassoldati, R. Grana, A. Cuoci, T. Faravelli, A.P. Kelley, C.K. Law, Hierarchical and comparative kinetic modeling of laminar flame speeds of hydrocarbon and oxygenated fuels, Progr. Energy Combust. Sci. 38 (2011) 468–582.
[43] F.N. Egolfopoulos, N. Hansen, Y. Ju, K. Kohse-Höinghaus, C.K. Law, F. Qi, Advances and challenges in laminar flame experiments and implications for combustion chemistry, Prog. Energy Combust. Sci. 43 (2014) 36–67.
[44] D. Razus, D. Oancea, C. Movileanu, Burning velocity evaluation from pressure evolution during the early stage of closed-vessel explosions, J. Loss Prev. Process Ind. 19 (2006) 334–342.
[45] D. Razus, V. Brinzea, M. Mitu, C. Movileanu, D. Oancea, Burning velocity of propane-air mixtures from pressure-time records during explosions in a closed spherical vessel, Energy Fuels 26 (2012) 901–909.
[46] M. Mitu, D. Razus, V. Giurcan, D. Oancea, Normal burning velocity and propagation speed of ethane–air: pressure and temperature dependence, Fuel 147 (2015) 27–34.
[47] COSILAB, 2012. Version 3.0.3, Rotexo-Softpredict-Cosilab GmbH & Co KG Bad Zwischenhahn.
[48] P.G. Hill, J. Hung, Laminar burning velocities of stoichiometric mixtures of methane with propane and ethane additives, Combust. Sci. Technol. 60 (1988) 7–30.
[49] I. Glassman, R. Yetter, Combustion, 4th ed., Elsevier, 2008 (Chapter 4).
[50] C.K. Law, Combustion Physics, Cambridge University Press, New York, 2006.
[51] C. Coné, C. Chauveau, I. Gokalp, D.F. Kurtulus, CO_2 addition and pressure effects on laminar and turbulent lean premixed CH_4 air flames, Proc. Combust. Inst. 32 (2009) 1803–1810.
[52] W. Qin, F.N. Egolfopoulos, T.T. Tsotsis, Fundamental and environmental aspects of landfill gas utilization for power generation, Chem. Eng. J. 82 (2001) 157–172.
[53] M. Liberman, Introduction to Chemistry and Physics of Combustion. Explosion, Flame, Detonation, Springer Verlag, 2008 (Chapter 5).
[54] R. Burke, F. Dewael, A. van Tiggelen, Kinetics of the propylene-oxygen flame reaction, Combust. Flame 7 (1963) 83–87.
[55] C. Movileanu, D. Razus, D. Oancea, Additive effects on the burning velocity of ethylene-air mixtures, Energy Fuels 25 (2011) 2444–2451.
[56] D. Razus, C. Movileanu, V. Branzea, D. Oancea, Overall activation parameters of propylene oxidation in premixed flames, Anal. Univ. Bucuresti Chimie 14 (I–II) (2005) 209–214.